Versão do arquivo anexado / Version of attached file:

Versão do Editor / Published Version

Mais informações no site da editora / Further information on publisher's website:

https://www.sciencedirect.com/science/article/pii/S0370269315009892

DOI: 10.1016/j.physletb.2015.12.041

Direitos autorais / Publisher's copyright statement:
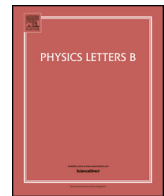
The transverse momentum dependence of charged kaon Bose–Einstein correlations in the SELEX experiment

The SELEX Collaboration

G.A. Nigmatkulov [i,*], A.K. Ponosov [i,1], U. Akgun [n], G. Alkhazov [j], J. Amaro-Reyes [l],
A. Asratyan [f], A.G. Atamantchouk [j,1], A.S. Ayan [n], M.Y. Balatz [f,1], A. Blanco-Covarrubias [l],
N.F. Bondar [j], P.S. Cooper [d], L.J. Dauwe [o,1], G.V. Davidenko [f], U. Dersch [g,3], A.G. Dolgolenko [f],
G.B. Dzyubenko [f,1], R. Edelstein [b], L. Emediato [q], A.M.F. Endler [c], J. Engelfried [l],
I. Eschrich [g,2], C.O. Escobar [q,4], N. Estrada [l], A.V. Evdokimov [f], I.S. Filimonov [h,1],
A. Flores-Castillo [l], F.G. Garcia [q,d], I. Giller [k], V.L. Golovtsov [j], P. Gouffon [q], E. Gülmez [a],
M. Iori [p], S.Y. Jun [b], M. Kaya [n,5], J. Kilmer [d], V.T. Kim [j], L.M. Kochenda [j], I. Konorov [g,6],
A.P. Kozhevnikov [e], A.G. Krivshich [j], H. Krüger [g,7], M.A. Kubantsev [f], V.P. Kubarovsky [e],
A.I. Kulyavtsev [b,d], N.P. Kuropatkin [j,d], V.F. Kurshetsov [e], A. Kushnirenko [b,e], J. Lach [d],
L.G. Landsberg [e,1], I. Larin [f], E.M. Leikin [h], G. López-Hinojosa [l], T. Lungov [q], V.P. Maleev [j],
D. Mao [b,8], P. Mathew [b,9], M. Mattson [b], V. Matveev [f], E. McCliment [n], M.A. Moinester [k],
V.V. Molchanov [e], A. Morelos [l], A.V. Nemitkin [h], P.V. Neoustroev [j], C. Newsom [n],
A.P. Nilov [f,1], S.B. Nurushev [e], A. Ocherashvili [k,10], Y. Onel [n], S. Ozkorucuklu [n,11], A. Penzo [r],
S.V. Petrenko [e], M. Procario [b,12], V.A. Prutskoi [f], B.V. Razmyslovich [j,13], D.A. Romanov [i],
V.I. Rud [h], J. Russ [b], J.L. Sánchez-López [l], A.A. Savchenko [i], J. Simon [g,14], G.V. Sinev [i,15],
A.I. Sitnikov [f], V.J. Smith [m], M. Srivastava [q], V. Steiner [k], V. Stepanov [j,13], L. Stutte [d],
M. Svoiski [j,13], V.V. Tarasov [f], N.K. Terentyev [j,b], I. Torres [l,16], L.N. Uvarov [j], A.N. Vasiliev [e],
D.V. Vavilov [e], E. Vázquez-Jáuregui [l,17], V.S. Verebryusov [f,1], V.A. Victorov [e],
V.E. Vishnyakov [f], A.A. Vorobyov [j], K. Vorwalter [g,18], J. You [b,d], R. Zukanovich-Funchal [q]

[a] *Bogazici University, Bebek 80815 Istanbul, Turkey*

* Corresponding author.
   E-mail address: nigmatkulov@gmail.com (G.A. Nigmatkulov).
[1] Deceased.
[2] Present address: University of California at Irvine, Irvine, CA 92697, USA.
[3] Present address: Advanced Mask Technology Center, Dresden, Germany.
[4] Present address: Instituto de Física da Universidade Estadual de Campinas, UNICAMP, SP, Brazil.
[5] Present address: Kafkas University, Kars, Turkey.
[6] Present address: Physik-Department, Technische Universität München, 85748 Garching, Germany.
[7] Present address: The Boston Consulting Group, München, Germany.
[8] Present address: Lucent Technologies, Naperville, IL, USA.
[9] Present address: Baxter Healthcare, Round Lake, IL, USA.
[10] Present address: NRCN, 84190 Beer-Sheva, Israel.
[11] Present address: Süleyman Demirel Universitesi, Isparta, Turkey.
[12] Present address: DOE, Germantown, MD, USA.
[13] Present address: Solidum, Ottawa, Ontario, Canada.
[14] Present address: Siemens Healthcare, Erlangen, Germany.
[15] Present address: Duke University, Durham, NC 27708, USA.
[16] Present address: Instituto Nacional de Astrofísica, Óptica y Electrónica, Tonantzintla, Mexico.
[17] Present address: SNOLAB, Canada.
[18] Present address: Allianz Insurance Group IT, München, Germany.

b *Carnegie–Mellon University, Pittsburgh, PA 15213, USA*
c *Centro Brasileiro de Pesquisas Físicas, Rio de Janeiro, Brazil*
d *Fermi National Accelerator Laboratory, Batavia, IL 60510, USA*
e *Institute for High Energy Physics, Protvino, Russia*
f *Institute of Theoretical and Experimental Physics, Moscow, Russia*
g *Max-Planck-Institut für Kernphysik, 69117 Heidelberg, Germany*
h *Moscow State University, Moscow, Russia*
i *National Research Nuclear University MEPhI (Moscow Engineering Physics Institute), Moscow, Russia*
j *Petersburg Nuclear Physics Institute, St. Petersburg, Russia*
k *Tel Aviv University, 69978 Ramat Aviv, Israel*
l *Universidad Autónoma de San Luis Potosí, San Luis Potosí, Mexico*
m *University of Bristol, Bristol BS8 1TL, United Kingdom*
n *University of Iowa, Iowa City, IA 52242, USA*
o *University of Michigan-Flint, Flint, MI 48502, USA*
p *University of Rome "La Sapienza" and INFN, Rome, Italy*
q *University of São Paulo, São Paulo, Brazil*
r *University of Trieste and INFN, Trieste, Italy*

ARTICLE INFO

ABSTRACT

We report the measurement of the one-dimensional charged kaon correlation functions using 600 GeV/c Σ^-, π^- and 540 GeV/c p beams from the SELEX (E781) experiment at the Fermilab Tevatron. $K^\pm K^\pm$ correlation functions are studied for three transverse pair momentum, k_T, ranges and parameterized by a Gaussian form. The emission source radii, R, and the correlation strength, λ, are extracted. The analysis shows a decrease of the source radii with increasing kaon transverse pair momentum for all beam types.

1. Introduction

In this paper we present results from $K^\pm K^\pm$ correlation femtoscopy study in 600 GeV/c $\Sigma^- C(Cu)$, $\pi^- C(Cu)$ and 540 GeV/c $pC(Cu)$ interactions from the SELEX (E781) experiment [1] at the Fermilab Tevatron. The correlation femtoscopy method allows to study spatio-temporal characteristics of the emission source at the level of 1 fm $= 10^{-15}$ m. The method is based on the Bose–Einstein enhancement of identical boson production at small relative momentum. The quantum statistics correlations were first observed as an enhanced production of the identical pion pairs with small opening angles in proton–antiproton collisions [2]. In 1960 this enhancement was explained by the symmetrization of the two-particle wave function by G. Goldhaber, S. Goldhaber, W.-Y. Lee, and A. Pais (GGLP effect) [3]. Later, in the 1970s, Kopylov and Podgoretsky suggested studying the interference effect in terms of the correlation function. They proposed the mixing technique to construct the uncorrelated reference sample, and clarified the role of the space–time characteristics of particle production [4–6]. Subsequently, two-particle correlations at small relative momentum were systematically studied for lepton–lepton [7], lepton-hadron [8], hadron–hadron [9], and heavy-ion [10,11] collisions. It was found that the system created in heavy-ion collisions undergoes the collective expansion and may be described by relativistic fluid dynamics [12–15]. By using the width of the quantum statistical enhancement, one can measure the radii R of the emitting source. The decrease of the extracted radii with increasing transverse pair momentum may be interpreted as the decrease of the "homogeneity lengths" [16] due to collective transverse flow.

A comparison of femtoscopic measurements in lepton and hadron-induced [17,18] collisions with heavy-ion collisions shows similar systematics [19,20]. These studies usually performed for pions. However, measurements of heavier particles may provide additional information about the size, orientation and dynamical timescales of the emission region.

2. Experimental setup and data selection

The SELEX (E781) detector is a three-stage magnetic spectrometer designed for charm hadroproduction study at $x_F > 0.1$ ($x_F = \frac{p_z}{p_{z_{max}}}$). We report the analysis of 1 billion events of 600 GeV/c $\Sigma^- C(Cu)$, $\pi^- C(Cu)$ and 540 GeV/c $p\,C(Cu)$ interactions recorded during the 1996–1997 fixed target run. About 2/3, 1/6 and 1/6 of the data were obtained on Σ^-, π^- and p beams, respectively.

The beam particle was identified as a meson or a baryon by a transition radiation detector. Interactions occurred on segmented targets, which consisted of 2 copper and 3 diamond foils separated by 1.5 cm clearance, and had a total thickness of 5% of an interaction length for protons. Particles were tracked in a set of 20 vertex Silicon Strip Detectors (SSD) arranged in 4 sets of planes with a strip pitch of 20–25 μm, rotated by 45°. Each of the detectors has a hit detection efficiency greater than 98%. Transverse vertex position resolution (σ) was 4 μm for the 600 GeV/c beam tracks. The average longitudinal vertex position resolution was 270 μm for primary vertex and 560 μm for secondary vertex. The detector geometry covers the forward 150 m rad cone. The particle momentum was measured by deflection of the track position by two magnets M1 and M2 in a system of proportional wire chambers and silicon strip detectors. Momentum resolution of a typical 100 GeV/c track was $\sigma_p/p \approx 0.5\%$. A Ring Imaging Cherenkov detector (RICH) performed particle identification in a wide momentum range and provided 2 σ K/π separation up to 165 GeV/c and single track ring radius resolution of 1.4% [21]. The kaon identification efficiency was over 90% above the kaon threshold (≈ 43 GeV/c). The average number of tracks reaching the RICH was about 5 per event [22]. The layout of the spectrometer is described elsewhere [1].
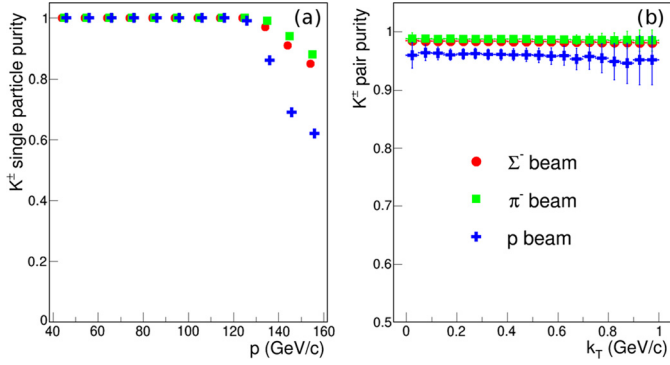
Fig. 1. Single $K^\pm$ purity as a function of momentum (a) and the average transverse pair momentum dependence of the $K^\pm$ pair purity for the Σ^- (circles), π^- (squares) and p (crosses) beams (b).

In this analysis we used primary tracks that have vertex silicon track segment matched with downstream segments measured in the M1 and M2 spectrometers, with the momentum from 45 to 160 GeV/c. In order to reduce the contamination of secondary particles, it was required that the extrapolated track distance to the primary vertex was less than 15 μm in the transverse plane. Only tracks that matched the RICH detector were used in the analysis. Charged kaons were identified with the likelihood to be a kaon at least three times exceeding any other particle hypothesis. Fig. 1(a) shows the single kaon purity as a function of the momentum for the Σ^-, π^- and p beams. It is defined as the fraction of the accepted kaon tracks that correspond to true kaon particles. The single particle purity was estimated from the RICH ring radius distributions of the data and by studying PYTHIA [23] simulations with the particle embedding through the detector. The main contamination for charged kaons in the momentum range $p > 120$ GeV/c comes from pions, because of the close ring radii in the RICH detector.

The electrons were eliminated from the analysis using the transition radiation detector (ETRD) that was placed before RICH. The contamination from other particle species in the studied momentum range is negligible. Fig. 1(b) shows the charged kaon pair purity as a function of the average transverse momentum of the pair obtained for the Σ^-, π^- and p beams. The $K^\pm$ pair purity is calculated as a product of two single-particle purities using the experimental momentum distributions.

After applying the cuts 4 842 147, 597 101 and 103 551 identical charged kaon pairs were selected for Σ^-, π^- and p beams, respectively.

3. Correlation femtoscopy

The two-particle correlation function is defined as the ratio of the probability to measure two particles with momenta $\vec{p}_1$ and $\vec{p}_2$ to their single particle probabilities:

$$C(\vec{p}_1, \vec{p}_2) = \frac{P(\vec{p}_1, \vec{p}_2)}{P(\vec{p}_1)P(\vec{p}_2)}. \tag{1}$$

Experimentally, one studies the correlation function $C(\vec{q}, \vec{K})$ in terms of relative momentum $\vec{q} = \vec{p}_1 - \vec{p}_2$ and average momentum $\vec{K} = (\vec{p}_1 + \vec{p}_2)/2$ of two particles:

$$C(\vec{q}, \vec{K}) = \frac{A(\vec{q}, \vec{K})}{B(\vec{q}, \vec{K})} \cdot D(\vec{q}, \vec{K}), \tag{2}$$

where $A(\vec{q}, \vec{K})$ is the measured distribution of relative momentum within the same event, $B(\vec{q}, \vec{K})$ is the reference or background distribution that is similar to the experimental distribution in all re-

spects except for the presence of femtoscopic correlations. The reference sample is usually formed from particles that come from different events (event mixing technique [6]). The quantity $D(\vec{q}, \vec{K})$ is a so-called correlation baseline that describes all non-femtoscopic correlations, such as, for instance, the correlations caused by the energy and momentum conservation-induced correlations [24]. In order to eliminate possible biases due to the construction of the reference samples, the measured correlation functions were corrected on the simulated distributions by constructing the double ratio:

$$R(Q) = \left(\frac{dN_{K^\pm K^\pm}/dQ}{dN_{ref}/dQ} \right) / \left(\frac{dN_{MC,K^\pm K^\pm}/dQ}{dN_{MC,ref}/dQ} \right), \tag{3}$$

where the subscripts "MC" and "MC, ref" correspond to the simulated data.

By virtue of the limited statistics available for the π^- and p beams, only the one-dimensional femtoscopic charged kaon analysis of correlation functions in terms of invariant relative momentum, $Q = \sqrt{(\vec{p}_1 - \vec{p}_2)^2 - (E_1 - E_2)^2}$, was performed. In order to extract the size of the emission region, R, one can use the Goldhaber parametrization. This assumes that the emitting source of identical bosons is described by a spherical Gaussian density function:

$$C(Q) = N\left(1 + \lambda e^{-R^2 Q^2}\right) \cdot D(Q), \tag{4}$$

where N is a normalization factor, λ describes the correlation strength, and $D(Q)$ is the baseline distribution. In the current analysis, the second order polynomial, $D(Q) = 1 + aQ + bQ^2$, was used for estimation of the baseline distribution. The momentum correlations of particles emitted at nuclear distances are also influenced by the effect of final-state interaction (FSI), Coulomb and strong interactions [25–28]. For identical kaons, the effect of strong interactions is negligible [29]. The correlation function of identical bosons should increase at low relative momentum, except for small values where Coulomb interaction becomes dominant. This may be taken into account by modifying Eq. (4):

$$C(Q) = N\left((1 - \lambda) + \lambda K(Q)\left(1 + e^{-R^2 Q^2}\right)\right) \cdot D(Q), \tag{5}$$

where the factor $K(Q)$ is the squared like-sign kaon pair Coulomb wave function integrated over a spherical Gaussian source [30–32].

4. Results and discussions

The results discussed in this Letter were obtained with the same detector setup, cuts and fitting procedures, giving an opportunity to compare the properties of the emission region for different hadron-induced collisions. The analysis was performed for three average transverse pair momentum $k_T = |\vec{p}_{T1} + \vec{p}_{T2}|/2$ ranges: (0.00–0.30), (0.30–0.55), (0.55–1.00) GeV/c and for the three beam types: Σ^-, π^-, p. The event mixing technique was used to construct the uncorrelated reference sample. Only events with two or more identical charged kaons, grouped by production target, were used in the event mixing. Kaons from adjacent events for each target were combined to provide an uncorrelated experimental background. Due to small differences in the measured correlation functions, the positive and negative kaon four-momentum distributions were combined in the numerator and the denominator before constructing the ratio. A purity correction was applied to the experimental correlation functions according to the expression:

$$C(Q) = \frac{C_{experimental}(Q) - 1}{P(Q)} + 1, \tag{6}$$
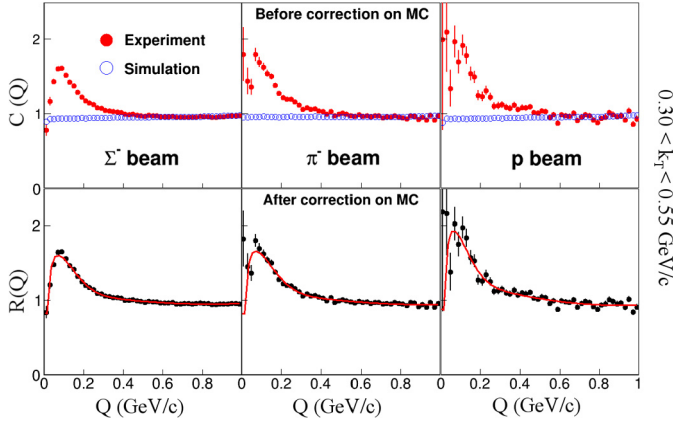
where $P(Q)$ is the pair purity.

Fig. 2. Top row shows the experimental (full circles) and PYTHIA-generated (open circles) correlation functions of identical kaons obtained from using the event mixed reference samples. The bottom row shows the fits to the double ratios according to Eq. (5). The second order polynomial was used for estimation of the non-femtoscopic effects. The correlation functions are measured for $0.30 < k_T < 0.55$ GeV/c range and columns from left to right represent the data obtained for Σ^-, π^- and p beams, respectively.

The top row of the Fig. 2 shows the experimental correlation functions (solid circles) after applying the purity correction measured in the $0.30 < k_T < 0.55$ GeV/c region for Σ^-, π^- and p beams. The correlation functions were normalized such that $C(Q) = 1$ for $0.5 < Q < 0.7$ GeV/c, where Bose–Einstein correlations are absent and the influence of the non-femtoscopic effects is small. The deviation of the correlation functions from unity at $Q > 0.7$ GeV/c corresponds to the non-femtoscopic correlations and the well-defined enhancement at $Q < 0.4$ GeV/c is due to the quantum statistical correlations. The Coulomb repulsion between like-sign kaons leads to the decrease of the correlation functions at $Q < 0.1$ GeV/c.

In order to correct for non-femtoscopic effects, the Monte Carlo event generator PYTHIA-6.4.28 [23] with different tunes (Perugia 0, Perugia 2010 and Perugia 2011 [33]) was used. PYTHIA contains neither Bose–Einstein correlations nor the final-state interactions. On the other hand, PYTHIA contains other kinematic effects, for instance, energy and momentum conservation effects, that could lead to baseline correlations. The Perugia 2011 tune, which best describes charged-particle multiplicity, was used as the main minimum-bias MC sample. The top row of the Fig. 2 shows the comparison of simulated correlation functions (empty circles), where PYTHIA events were filtered through the analysis cuts, with the experimental distributions (solid circles) measured for $0.30 < k_T < 0.55$ GeV/c range. The PYTHIA-generated correlation functions were normalized in the same way as the experimental correlation functions.

It is seen that PYTHIA qualitatively describes the experimental baseline in the region $Q > 0.5$ GeV/c, where the effect of femtoscopic correlations is negligible. Since the MC calculation does not include wave function symmetrization for identical particles, the femtoscopic peak at low relative four-momentum region, $Q < 0.4$ GeV/c, is absent.

The bottom row of the Fig. 2 shows double ratios, where the experimental correlation functions are divided by the PYTHIA-generated ones, obtained for the Σ^-, π^- and p beams in the $0.30 < k_T < 0.55$ GeV/c region. The double ratios were fitted using Eq. (5). In the current analysis, the Coulomb function $K(Q)$ was integrated over a spherical source of 1 fm. Due to imperfections of the simulation in the $Q > 0.7$ GeV/c region, the non-femtoscopic term $D(Q) = 1 + aQ + bQ^2$ was used.
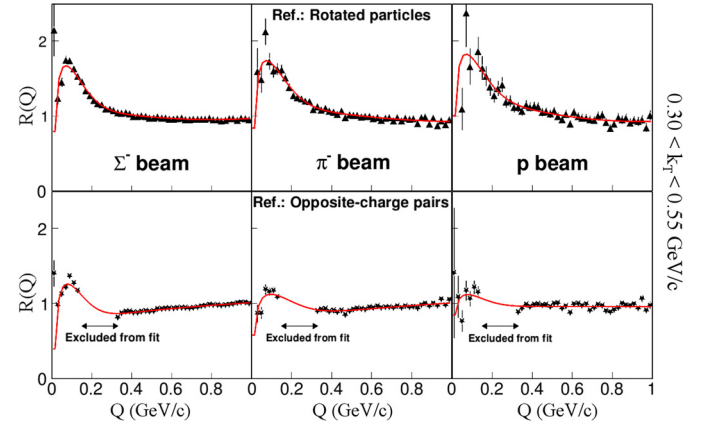

Fig. 3. The correlation functions constructed with rotated particles (top panel) and opposite-charge pairs (bottom panel) for $0.30 < k_T < 0.55$ GeV/c range. The range $0.19 < Q < 0.35$ GeV/c on the bottom panel is excluded from fits due to the contribution from the $\phi(1020)$ meson decay. The fits were performed using Eq. (5). The columns represent Σ^- (left), π^- (middle) and p (right) beams.

Table 1
Systematic uncertainty (minimal and maximal) values for different sources of systematic uncertainty (in percent). The values of minimum (maximum) uncertainty can be from different average transverse pair momentum range or the beam type, but from a specific source.

The systematic uncertainty source	λ (%)	R (%)
Event/particle selection	1–7	1–9
PID and purity	0–4	0–6
Fit range	1–5	1–4
Momentum resolution	0–1	0–1
Two-track effects	–	–
Non-femtoscopic form	0–4	1–11
Coulomb function	–	–
Reference sample	1–8	5–13
Total	2–13	5–21

To estimate the influence of choice of the reference sample, the different methods of constructing uncorrelated charged particle distributions were used: *opposite-charge pairs* and *rotated particles*, where pairs are constructed after inverting the x and y components of the three-momentum of one of the two particles. Fig. 3 shows the double ratios obtained from using rotated particles (top panel) and opposite-charge pairs (bottom panel) reference samples. The double ratios were fitted using Eq. (5); and the second order polynomial, $D(Q) = 1 + aQ + bQ^2$, was used to describe the non-femtoscopic term. It was found that the extracted femtoscopic parameters, λ and R, obtained from using rotated particles reference samples are similar to those from the event mixed ones.

The reference samples constructed from the opposite-charge kaon pairs contain peaks coming from strong resonance decays; and are influenced by the Coulomb attraction at $Q < 0.1$ GeV/c. The magnitudes of the resonance peaks measured for the real and simulated correlation functions were found to be different. This can be explained by the absence of the final-state rescattering of particles in PYTHIA. The double ratios obtained for unlike-sign kaon pairs were fitted the same way as the event mixed ones. The range $0.19 < Q < 0.35$ GeV/c was excluded from fits due to the $\phi(1020)$ meson decay and because the influence of the final-state interactions between opposite-charge kaon pairs was not taken into account.

The different sources of systematic uncertainties were studied for each k_T range and beam type. Table 1 shows the maximal and minimal values of systematic uncertainty that correspond to specific uncertainty sources. The values of the total uncertainty are

Table 2

$K^{\pm}K^{\pm}$ source parameters for Σ^-, π^- and p beams. Statistical and systematic uncertainties are presented.

Beam type	k_T (GeV/c)	χ^2/N_{dof}	N	λ	R (fm)	a (GeV/c^{-1})	b (GeV/c^{-2})
Σ^-	(0.00–0.30)	126/45	1.23 ± 0.01	$0.71 \pm 0.02 \pm 0.08$	$1.32 \pm 0.02 \pm 0.07$	-0.59 ± 0.02	0.38 ± 0.02
	(0.30–0.55)	85/45	1.18 ± 0.01	$0.66 \pm 0.02 \pm 0.08$	$1.18 \pm 0.02 \pm 0.05$	-0.47 ± 0.03	0.28 ± 0.02
	(0.55–1.00)	142/45	1.05 ± 0.03	$0.66 \pm 0.04 \pm 0.10$	$0.98 \pm 0.03 \pm 0.04$	-0.22 ± 0.08	0.13 ± 0.05
π^-	(0.00–0.30)	62/45	1.19 ± 0.03	$0.67 \pm 0.06 \pm 0.09$	$1.25 \pm 0.06 \pm 0.06$	-0.49 ± 0.07	0.31 ± 0.05
	(0.30–0.55)	66/45	1.21 ± 0.04	$0.69 \pm 0.06 \pm 0.06$	$1.13 \pm 0.06 \pm 0.06$	-0.46 ± 0.09	0.24 ± 0.07
	(0.55–1.00)	58/45	1.34 ± 0.07	$0.44 \pm 0.10 \pm 0.11$	$1.16 \pm 0.19 \pm 0.14$	-0.71 ± 0.09	0.42 ± 0.09
p	(0.00–0.30)	65/45	1.51 ± 0.06	$0.98 \pm 0.17 \pm 0.13$	$1.54 \pm 0.16 \pm 0.17$	-0.97 ± 0.10	0.62 ± 0.08
	(0.30–0.55)	62/45	1.39 ± 0.12	$0.80 \pm 0.15 \pm 0.13$	$1.32 \pm 0.12 \pm 0.15$	-0.72 ± 0.13	0.40 ± 0.11
	(0.55–1.00)	43/44	1.26 ± 0.16	$0.91 \pm 0.24 \pm 0.11$	$1.13 \pm 0.17 \pm 0.11$	-0.61 ± 0.31	0.37 ± 0.24

not necessarily equal to the quadratic sum of all the uncertainties due to the fact that they can come from different beam types or average transverse pair momentum ranges.

The uncertainty due to the fit range was estimated by varying the upper limit of the fit from $Q = 1$ GeV/c to $Q = 0.6$ GeV/c. The lowest value of the upper limit of the fit range corresponds to the end of the correlation region. Changing the radius of the Coulomb source in the range from 0.5 fm to 1.5 fm has negligible effect on the extracted emitting source parameters.

Different baseline shapes [34–36] were used to estimate the systematic uncertainty due to the baseline determination:

$$D(Q) = 1, \tag{7}$$

$$D(Q) = 1 + aQ, \tag{8}$$

$$D(Q) = 1 + e^{-aQ^2}, \tag{9}$$

$$D(Q) = \sqrt{1 + aQ^2 + bQ^4}. \tag{10}$$

The smearing of single particle momenta was studied by embedding simulated kaon tracks with known momenta through the detector. Experimental correlation functions were corrected for momentum resolution using the expression:

$$C_{corr}(Q) = \frac{C_{uncorr}(Q)C_{unsmeared}(Q)}{C_{smeared}(Q)}, \tag{11}$$

where $C_{corr}(Q)$ is the corrected correlation function and $C_{uncorr}(Q)$ represents the measured correlation function. The $C_{unsmeared}(Q)$ and $C_{smeared}(Q)$ are the correlation functions without and with taking into account the momentum resolution effect, respectively. The smearing of the single particle momenta leads to the smearing of the correlation function in the $Q < 0.2$ GeV/c range. This decreases the amplitude of the peak and makes it wider. The systematic uncertainty of this effect does not exceed 1%. The two-track reconstruction effects: "merging", when two tracks are reconstructed as one; and "splitting", when one track is reconstructed as two, were studied and found to be negligible.

The main systematic uncertainty arises from using different methods of constructing the uncorrelated reference sample. The dominant contribution comes from using opposite-charge kaon pairs. The contamination of the "reference sample" uncertainty from using different PYTHIA tunes does not exceed 5%.

The systematic errors on R and λ for each beam type and k_T range are taken as the rms spread of the values obtained for the different sources of systematic uncertainty.

The results of fits of $R(Q)$ based on the parametrization of Eq. (5) with $D(Q) = 1 + aQ + bQ^2$ are given in Table 2. The extracted source radii and correlation strength for Σ^- (circles), π^- (squares) and p (stars) beams as a function of transverse pair momentum are shown in Figs. 4(a) and 4(b), respectively. The source radii slightly decrease with increasing k_T for all the beam types, except the highest average transverse pair momentum interval for
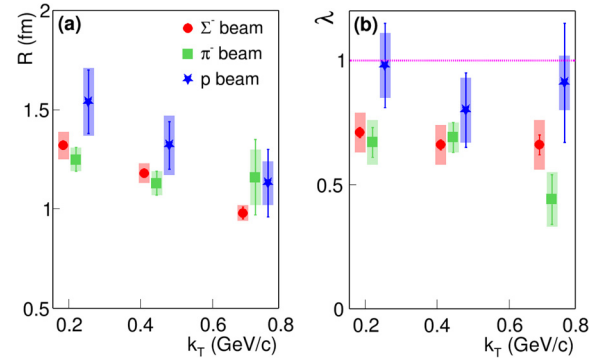

Fig. 4. $K^{\pm}K^{\pm}$ source parameters R (a) and λ (b) measured for Σ^- (circles), π^- (squares) and p (stars) beams as a function of transverse pair momentum, k_T. Statistical (lines) and systematic (boxes) uncertainties are shown.

the π^- beam. The femtoscopic radii measured for Σ^-, π^- and p beams are consistent within the uncertainties. The small difference between measured source parameters probably arises from different contamination from resonance decays [37].

The decrease of the source radii with transverse pair momentum was previously observed in heavy-ion collisions and interpreted as a collective hydrodynamic behavior (collective flow) [38, 39]. The first direct comparison of correlation femtoscopy in $p + p$ and heavy-ion collisions under the same detector conditions, reconstruction, analysis and fitting procedures was performed by the STAR collaboration [20]. It was shown that $p + p$ collisions also have the transverse momentum scaling. Although the interpretation of these results is still unclear, the similarities could indicate a connection between the underlying physics.

The transverse momentum dependence was also observed for $\pi\pi$ in e^+e^- [40,41] and pp collisions [20,35,42]. For the first time a similar analysis of charged kaon Bose–Einstein correlations for more than one transverse pair momentum and multiplicity range was recently performed by the ALICE collaboration at the LHC in pp collisions at $\sqrt{s} = 7$ TeV [34]. It was shown that charged kaon femtoscopic radii decrease with transverse pair momentum for middle and high multiplicity ranges.

There are several possible processes that may lead to the k_T dependencies in the hadronic collisions:

1. The space–momentum dependence of the femtoscopic radii may be generated by long-lived resonances [43]. In particular this may play a significant role in high multiplicity bins, where the bulk collective flow is predicted [44].

2. Humanic's model [45], based on space–time geometry of hadronization and effects of final-state rescattering between hadrons, reproduces both multiplicity and transverse mass dependence measured at the Tevatron [46].

3. In small systems, the string fragmentation should generate momentum and space correlations, such as k_T dependence of the

source radii. However, there are almost no quantitative predictions that may be directly compared with data except the τ-model in which space–time and momentum space are strongly correlated [47]. Moreover, the Lund string model is not able to reproduce the mass dependence of the radii [17,48–50].

4. Hydrodynamic bulk collective flow may lead to a k_T dependence that is very similar to that from heavy-ion collisions.

Taking the aforementioned possibilities, the origin of the transverse pair momentum dependence of the femtoscopic radii in hadronic collisions is still unclear. Further theoretical studies are needed in order to understand the underlying physics.

5. Summary

Charged kaon Bose–Einstein correlations were measured in the SELEX experiment. One-dimensional charged kaon correlation functions in terms of the invariant four-momentum difference were constructed for Σ^-, π^- and p beams and three transverse pair momentum ranges: (0.00–0.30), (0.30–0.55) and (0.55–1.00) GeV/c. The source parameters of correlation strength, λ, and source radii, R, were extracted for all beam types and for the three average transverse pair momentum ranges. The slight decrease of the femtoscopic radii with pair transverse momentum was observed for all three beam types, except for the highest k_T range of the π^- beam. The values of the emitting source radii obtained for Σ^-, π^- and p beams are consistent within the uncertainties.

Acknowledgements

References

[1] J.S. Russ, N. Akchurin, V.A. Andreev, et al., First charm hadroproduction results from SELEX, in: ICHEP'98 Proc. Int. Conf. on High Energy Physics II, 1998, p. 1259, arXiv:hep-ex/9812031.

[2] G. Goldhaber, W.B. Fowler, S. Goldhaber, T.F. Hoang, T.E. Kalogeropoulos, W.M. Powell, Pion–pion correlations in antiproton annihilation events, Phys. Rev. Lett. 3 (1959) 181–183.

[3] G. Goldhaber, S. Goldhaber, W. Lee, A. Pais, Influence of Bose–Einstein statistics on the antiproton–proton annihilation process, Phys. Rev. 120 (1960) 300–312.

[4] G.I. Kopylov, M.I. Podgoretsky, Correlations of identical particles emitted by highly excited nuclei, Sov. J. Nucl. Phys. 15 (1972) 219–223.

[5] G.I. Kopylov, M.I. Podgoretsky, Multiple production and interference of particles emitted by moving sources, Sov. J. Nucl. Phys. 18 (1974) 336–341.

[6] G.I. Kopylov, Like particle correlations as a tool to study the multiple production mechanism, Phys. Lett. B 50 (1974) 472–474.

[7] G. Abbiendi, et al., Transverse and longitudinal Bose–Einstein correlations in hadronic Z^0 decays, Eur. Phys. J. C 16 (2000) 423–433, arXiv:hep-ex/0002062.

[8] S. Chekanov, et al., Bose–Einstein correlations in one and two dimensions in deep inelastic scattering, Phys. Lett. B 583 (2004) 231–246, arXiv:hep-ex/0311030.

[9] K. Aamodt, et al., Two-pion Bose–Einstein correlations in pp collisions at $\sqrt{s} = 900$ GeV, Phys. Rev. D 82 (2010) 052001, arXiv:1007.0516.

[10] H. Beker, et al., m_T dependence of boson interferometry in heavy ion collisions at the CERN SPS, Phys. Rev. Lett. 74 (1995) 3340–3343.

[11] L. Adamczyk, et al., Beam-energy-dependent two-pion interferometry and the freeze-out eccentricity of pions measured in heavy ion collisions at the STAR detector, Phys. Rev. C 92 (2015) 014904, arXiv:1403.4972 [nucl-ex].

[12] J. Adams, et al., Experimental and theoretical challenges in the search for the quark–gluon plasma: the STAR Collaboration's critical assessment of the evidence from RHIC collisions, Nucl. Phys. A 757 (2005) 102–183, arXiv:nucl-ex/0501009.

[13] K. Adcox, et al., Formation of dense partonic matter in relativistic nucleus–nucleus collisions at RHIC: experimental evaluation by the PHENIX Collaboration, Nucl. Phys. A 757 (2005) 184–283, arXiv:nucl-ex/0410003.

[14] B.B. Back, et al., The PHOBOS perspective on discoveries at RHIC, Nucl. Phys. A 757 (2005) 28–101, arXiv:nucl-ex/0410022.

[15] I. Arsene, et al., Quark–gluon plasma and color glass condensate at RHIC? The perspective from the BRAHMS experiment, Nucl. Phys. A 757 (2005) 1–27, arXiv:nucl-ex/0410020.

[16] S.V. Akkelin, Y.M. Sinyukov, The HBT-interferometry of expanding sources, Phys. Lett. B 356 (1995) 525–530.

[17] G. Alexander, I. Cohen, E. Levin, The dependence of the emission size on the hadron mass, Phys. Lett. B 452 (1999) 159–166, arXiv:hep-ph/9901341.

[18] W. Kittel, Bose–Einstein correlations in Z fragmentation and other reactions, Acta Phys. Pol. B 32 (2001) 3927–3972, arXiv:hep-ph/0110088.

[19] Z. Chajęcki, Femtoscopy in hadron and lepton collisions: RHIC results and world systematics, Acta Phys. Pol. B 40 (2009) 1119–1136, arXiv:0901.4078.

[20] M.M. Aggarwal, et al., Pion femtoscopy in $p + p$ collisions at $\sqrt{s} = 200$ GeV, Phys. Rev. C 83 (2011) 064905, arXiv:1004.0925.

[21] J. Engelfried, et al., The SELEX phototube RICH detector, Nucl. Instrum. Methods A 431 (1999) 53–69, arXiv:hep-ex/9811001.

[22] J. Engelfried, et al., The E781 (SELEX) RICH detector, Nucl. Instrum. Methods A 409 (1998) 439–442.

[23] T. Sjöstrand, S. Mrenna, P. Skands, PYTHIA 6.4 physics and manual, J. High Energy Phys. 05 (2006) 026, arXiv:hep-ph/0603175v2.

[24] Z. Chajęcki, M. Lisa, Global conservation laws and femtoscopy of small systems, Phys. Rev. C 78 (2008) 064903, arXiv:0803.0022.

[25] R. Lednický, V.L. Lyuboshitz, B. Erazmus, D. Nouais, How to measure which sort of particles was emitted earlier and which later, Phys. Lett. B 373 (1996) 30–34.

[26] S. Voloshin, R. Lednický, S. Panitkin, N. Xu, Relative space–time asymmetries in pion and nucleon production in noncentral nucleus–nucleus collisions at high-energies, Phys. Rev. Lett. 79 (1997) 4766–4769, arXiv:nucl-th/9708044.

[27] S. Pratt, Shapes and sizes from non-identical-particle correlations, Braz. J. Phys. 37 (2007) 871–876, arXiv:nucl-th/0612006.

[28] R. Lednický, Finite-size effect on two-particle production, J. Phys. G, Nucl. Part. Phys. 35 (2008) 125109.

[29] R. Lednický, V.V. Lyuboshitz, V.L. Lyuboshitz, Final-state interactions in multi-channel quantum systems and pair correlations of nonidentical and identical particles at low relative velocities, Phys. At. Nucl. 61 (1998) 2050–2063.

[30] M.G. Bowler, Coulomb corrections to Bose–Einstein corrections have greatly exaggerated, Phys. Lett. B 270 (1991) 69–74.

[31] Y. Sinyukov, R. Lednický, S.V. Akkelin, J. Pluta, B. Erazmus, Coulomb corrections to Bose–Einstein corrections have greatly exaggerated, Phys. Lett. B 432 (1998) 248–257.

[32] J. Adams, et al., Pion interferometry in $Au + Au$ collisions at $\sqrt{s_{NN}} = 200$ GeV, Phys. Rev. C 71 (2005) 044906, arXiv:nucl-ex/0411036.

[33] P.Z. Skands, Tuning Monte Carlo generators: the Perugia tunes, Phys. Rev. D 82 (2010) 074018, arXiv:1005.3457.

[34] B. Abelev, et al., Charged kaon femtoscopic correlations in pp collisions at $\sqrt{s} = 7$ TeV, Phys. Rev. D 87 (2013) 052016, arXiv:1212.5958v2.

[35] V. Khachatryan, et al., Measurement of Bose–Einstein correlations in pp collisions at $\sqrt{s} = 0.9$ and 7 TeV, J. High Energy Phys. 05 (2011) 029, arXiv:1101.3518.

[36] S.V. Akkelin, Y.M. Sinyukov, Deciphering nonfemtoscopic two-pion correlations in $p + p$ collisions with simple analytical models, Phys. Rev. D 85 (2012) 074023, arXiv:1106.5120.

[37] R. Lednický, T.B. Progulova, Influence of resonances on Bose–Einstein correlations of identical pions, Z. Phys. C 55 (1992) 295–305.

[38] M. Lisa, S. Pratt, R. Soltz, U. Wiedemann, Femtoscopy in relativistic heavy ion collisions: two decades of progress, Annu. Rev. Nucl. Part. Sci. 55 (2005) 357–402, arXiv:nucl-ex/0505014.

[39] S. Pratt, Pion interferometry for exploding sources, Phys. Rev. Lett. 53 (1984) 1219–1221.

[40] G. Abbiendi, et al., Bose–Einstein study of position–momentum correlations of charged pions in hadronic Z^0 decays, Eur. Phys. J. C 52 (2007) 787–803, arXiv:0708.1122.

[41] P. Achard, et al., Test of the τ-model of Bose–Einstein correlations and reconstruction of the source function in hadronic Z-boson decay at LEP, Eur. Phys. J. C 71 (2011) 1648, arXiv:1105.4788.

[42] K. Aamodt, et al., Femtoscopy of pp collisions at $\sqrt{s} = 0.9$ and 7 TeV at the LHC with two-pion Bose–Einstein correlations, Phys. Rev. D 84 (2011) 112004, arXiv:1101.3665.

[43] U.A. Wiedemann, U.W. Heinz, Resonance contributions to Hanbury-Brown–Twiss correlation radii, Phys. Rev. C 56 (1997) 3265–3286, arXiv:nucl-th/9611031.

[44] K. Werner, I. Karpenko, T. Pierog, M. Bleicher, K. Mikhailov, Evidence for hydrodynamic evolution in proton–proton scattering at 900 GeV, Phys. Rev. C 83 (2011) 044915, arXiv:1010.0400.

[45] T.J. Humanic, Predictions for two-pion correlations for $\sqrt{s} = 14$ TeV proton–proton collisions, Phys. Rev. C 76 (2007) 025205, arXiv:nucl-th/0612098.

[46] T. Alexopoulos, et al., Study of source size in $p\bar{p}$ collisions at $\sqrt{s} = 1.8$ TeV using pion interferometry, Phys. Rev. D 48 (1993) 1931–1942.

[47] T. Csorgő, W. Kittel, W.J. Metzger, T. Novák, Parametrization of Bose–Einstein correlations and reconstruction of the space–time evolution of pion production in e^+e^- annihilation, Phys. Lett. B 663 (2008) 214–216, arXiv:0803.3528.

[48] A. Bialas, M. Kucharczyk, H. Palka, K. Zalewski, Mass dependence of HBT correlations in e^+e^- annihilation, Phys. Rev. D 62 (2000) 114007, arXiv:hep-ph/0006290.

[49] G. Alexander, Open questions related to Bose–Einstein correlations in $e^+e^- \rightarrow$ hadrons, Acta Phys. Pol. B 35 (2004) 69–76, arXiv:hep-ph/0311114.

[50] G. Alexander, Mass and transverse mass effects on the hadron emitter size, Phys. Lett. B 506 (2001) 45–51, arXiv:hep-ph/0101319.